



Published in final edited form as:

*Hear Res.* 2013 October ; 304: 153–158. doi:10.1016/j.heares.2013.07.007.

## The efficiency of design-based stereology in estimating spiral ganglion populations in mice

Amy E. Schettino<sup>a,b</sup> and Amanda M. Lauer<sup>a,†</sup>

<sup>a</sup>Center for Hearing and Balance, Dept. of Otolaryngology-Head & Neck Surgery, Johns Hopkins University, Baltimore, MD

<sup>b</sup>Undergraduate Program in Neuroscience, Zanvyl Kreiger School of Arts and Sciences, Johns Hopkins University, Baltimore, MD

### Abstract

Accurate quantification of cell populations is essential in assessing and evaluating neural survival and degeneration in experimental groups. Estimates obtained through traditional two-dimensional counting methods are heavily biased by the counting parameters in relation to the size and shape of the neurons to be counted, resulting in a large range of inaccurate counts. In contrast, counting every cell in a population can be extremely labor-intensive. The present study hypothesizes that design-based stereology provides estimates of the total number of cochlear spiral ganglion neurons (SGNs) in mice that are comparable to those obtained by other accurate cell-counting methods, such as a serial reconstruction, while being a more efficient method. SGNs are indispensable for relaying auditory information from hair cells to the auditory brainstem, and investigating factors affecting their degeneration provides insight into the physiological basis for the progression of hearing dysfunction. Stereological quantification techniques offer the benefits of efficient sampling that is independent of the size and shape of the SGNs. Population estimates of SGNs in cochleae from young C57 mice with normal-hearing and C57 mice with age-related hearing loss were obtained using the optical fractionator probe and traditional two-dimensional counting methods. The average estimated population of SGNs in normal-hearing mice was 7009, whereas the average estimated population in mice with age-related hearing loss was 5096. The estimated population of SGNs in normal-hearing mice fell within the range of values previously reported in the literature. The reduction in the SGN population in animals with age-related hearing loss was statistically significant. Stereological measurements required less time per section compared to two-dimensional methods while optimizing the amount of cochlear tissue analyzed. These findings demonstrate that design-based stereology provides a practical alternative to other counting methods such as the Abercrombie correction method, which has been shown to notably underestimate cell populations, and labor-intensive protocols that account for every cell individually.

### Keywords

stereology; cell counting; cochlea; spiral ganglion neuron; mouse; hearing loss

---

© 2013 Elsevier B.V. All rights reserved.

<sup>†</sup>Corresponding author: 515 Traylor Building, 720 Rutland Ave., Johns Hopkins University, Baltimore, MD 21205, 240-481-4035 (cell), 443-287-6336 (office), 443-287-6338 (lab), alauer2@jhmi.edu.

**Publisher's Disclaimer:** This is a PDF file of an unedited manuscript that has been accepted for publication. As a service to our customers we are providing this early version of the manuscript. The manuscript will undergo copyediting, typesetting, and review of the resulting proof before it is published in its final citable form. Please note that during the production process errors may be discovered which could affect the content, and all legal disclaimers that apply to the journal pertain.

## 1. Introduction

Comparing cell populations is an essential tool in assessing neural survival and degeneration in experimental groups. In order to evaluate the extent and significance of such survival and degeneration, accurate methods of quantification of neuronal populations are needed. Spiral ganglion neurons (SGNs) of the cochlea are indispensable in relaying auditory information from hair cells to the auditory brainstem, and studying their survival and degeneration provides insight into the physiological basis for the progression of hearing loss. Despite decades of research, techniques for quantifying the number of SGNs in a cochlea remains quite varied across studies (Richter et al., 2011).

Current cell counting techniques include three-dimensional serial reconstruction, two-dimensional cell body profile counts often with assumption-based correction factors, and stereological analysis. Serial reconstructions of three-dimensional tissue volumes most accurately determine population size but require an extremely labor-intensive process because they account for each cell individually. This method requires an observer to count every cell in the first section, then overlay the image of the second section and count all cells that do not appear in the first section. This process repeats until all cells have been accounted for and uses every section from the region under study. A three-dimensional view of the cochlea may also be constructed using specialized protocols with confocal microscopy and thin-sheet laser imaging microscopy (Johnson et al., 2011; MacDonald and Rubel, 2008, 2010). Two-dimensional profile counts vary widely depending on the parameters used, such as section thickness, and reflect estimates of cross-sectional profiles rather than of the actual population. These methods are particularly vulnerable to variation in neuron size and shape, and many studies report a raw count of SGNs without applying any sort of correction factor. However, even studies that employ assumption-based methods, usually two-dimensional profile counts with the assumption-based Abercrombie correction factor, which multiplies profile counts by a correction factor based on an assumed neuronal diameter, consistently underestimate SGN counts by 44%, possibly from variation in cell shape and orientation and uneven tissue shrinkage (Mouton, 2001; Guillery, 2002; Ishiyama et al., 2011). This problem can be compounded by changes in cell size and shape that may occur during neural degeneration, regeneration, and recovery. For instance, the addition of exogenous neurotrophins in response to hearing loss results in SGN survival and also an increase in SGN soma size, emphasizing the need for a counting method unaffected by such changes (Glueckert et al., 2008; Shepherd et al, 2008).

Stereological methods are the least prevalent approach but may offer an efficient and accurate alternative. Design-based stereology, also called unbiased stereology, is an analytical tool that is used to quantify populations of naturally occurring three-dimensional objects based on their two-dimensional cross sections. Unlike biased counting methods, estimates obtained by stereological methods are not significantly affected by the counting parameters used or the size and shape of the cell and increased sampling improves precision rather than further confounding the data. In order to sample efficiently without sacrificing accuracy, stereology must avoid double-counting objects in the small areas under evaluation. It minimizes this error in a two-dimensional plane by setting a standardized counting frame around each counting site and in the third dimension by comparing two such parallel planes, whether optical or physical. The physical disector and the optical disector are two methods that apply these stereological principles to cell counting. The physical disector relies on precisely aligning images of two adjacent serial sections and ensuring that all cells are counted once, without double counting the cells that appear in both sections. Although the process is similar to a serial reconstruction, the physical disector only requires a sample of pairs of adjacent sections, rather than all sections from the region of interest. The optical disector, used in the present study, removes the need for adjacent sections since the observer

scrolls between two optical planes within a single thick section and marks each cell that comes into focus. During this analysis, measurements are taken that enable observers to detect tissue shrinkage or deformation and appropriately accommodate such irregularities to minimize bias (Dorph-Petersen et al., 2001).

Ideally, researchers should adopt a method of quantifying SGNs that strikes a balance between practicality and accuracy. Certain methods will be most practical for a particular study. Counting all neurons within Rosenthal's canal using unbiased techniques will undoubtedly result in the most accurate data (Richter et al., 2011). The total number of SGNs is often not the only measure of interest, but rather one of a number of anatomical and functional measures within a study. For instance, thick osmicated cross sections through the cochlea may be collected with the intention of selecting small pieces of tissue for electron microscopic evaluation (e.g., Lauer et al., 2012; Stamatakis et al., 2006) or evaluating the status of both neural and non-neural cochlear structures in a mutant mouse model (e.g., Hequembourg and Liberman, 2001; Ohlemiller and Gagnon, 2007). In such cases, counting every neuron is not necessarily practical or necessary. The present study aims to demonstrate that design-based stereology accurately estimates the total number of cochlear SGNs in mice using assumption-free methods, while being more efficient than a serial reconstruction. This study also suggests that design-based stereology is sensitive to hearing loss-related SGN degeneration by comparing stereological SGN counts in young normal-hearing C57Bl/6J (C57) mice to counts from old C57 mice, a strain that has a well-characterized genetic predisposition to age-related hearing loss and cochlear degeneration (Mikaelian, 1979; Li and Borg, 1991; Francis et al., 2003; Hequembourg and Liberman, 2001). This technique is applicable to other animal models as well.

The optical disector stereological probe calculates an estimate by counting cells from a fraction of the sections spanning a region of interest. Objects that come into focus between the top and bottom optical planes of that section are counted, and varying the section thickness or section fraction does not affect final population estimate, as it would in profile counting. This reduces the number of sections required for analysis compared to the serial reconstruction method that requires analysis of every section. Some recent studies have opted to compare two-dimensional SGN densities; however, this cannot be used to estimate the total population. We describe a procedure for using the optical fractionator probe and compare it to other methods of estimating SGN populations in mice.

## 2. Materials and Methods

### 2.1 Subjects

Adult C57 mice were anesthetized with ketamine and xylazine in ethanol and perfused intracochlearly with 1% osmium tetroxide in 1% potassium ferricyanide, decalcified, dehydrated in graded alcohols, and embedded in Araldite as part of previous experiments (Francis et al., 2003; Stamatakis et al., 2006). The cochleae were sectioned at 40  $\mu\text{m}$  parallel to the modiolus, then mounted between sheets of Aclar and analyzed using the procedures described below. The reader is referred to those papers for more detailed descriptions of tissue harvest and preparation techniques. Four cochleae were analyzed from young mice ages 8 to 11 weeks old, and four cochleae were analyzed from mice 8 to 11.5 months old. All subjects appeared healthy, with normal respiratory activity, normal tympanic membranes, and with no evidence of external or middle ear infection at the time of tissue harvest. All animal procedures were performed in accordance with the Guide for the Care and Use of Laboratory Animals and with the approval of the Animal Care and Use Committee of the Johns Hopkins University School of Medicine.

## 2.2 Stereology

Though we performed the stereological analysis on osmicated tissue samples, the basic procedures described here can be applied to cochlear sections prepared using other neuron stains such as haematoxylin-eosin, toluidine blue, or with unstained tissue visualized using differential interference contrast (Nomarski) or phase contrast microscopy. SGNs were counted using the Optical Fractionator Probe in the StereoInvestigator (SI) software (Microbrightfield Bioscience, Williston, VT) using parameters determined by a pilot study and based on those described by Camerero et al. (2011). The reader is referred to the online Optical Fractionator Probe workflow webinar available for download at [www.mbfbioscience.com](http://www.mbfbioscience.com) for a tutorial explaining how to use the software. Similar procedures may be used with the Optical Fractionator probe included with other commercially available stereology systems such as Stereologer. The area sampling fraction (asf) was calculated from a sampling grid of  $120 \times 120 \mu\text{m}$  and counting frame of  $36 \times 40 \mu\text{m}$ , height and width respectively, for an asf of  $1/10$ . Every other section was used for counting, thus the section sampling fraction (ssf) was  $1/2$ . The evaluation interval was set to  $20 \mu\text{m}$  of sections originally cut at a thickness of  $40 \mu\text{m}$ . Using the SI software, the region of interest, Rosenthal's canal, was traced at  $40\times$  magnification, then the sampling grid was placed over the region of interest and counting sites were selected randomly by the software program. At each counting site, an observer measured the top and bottom of the section by scrolling entirely through the section and recording the depth at which any object in the grid first came into focus. The tops of cell bodies were marked if they came into focus within the evaluation interval and appeared within the counting frame or touched the green boundaries, but not the red boundaries, as shown in Figure 1. All counts were performed using a Heidenhain motorized microscope stage, Optronics video camera, Nikon E500 microscope, Nikon CFIUW  $10\times/25$  eyepiece, and a high-quality Nikon Plan Apo  $40\times/0.95$  objective with cover glass adjustment gauge. The microscope condensers and lighting were adjusted to achieve Kohler illumination to provide optimum contrast ([www.microscopyu.com](http://www.microscopyu.com)).

## 2.3 Two-dimensional SGN Density Counts

Two-dimensional SGN density was measured by counting SGNs that appeared within a randomly placed two-dimensional  $50\mu\text{m} \times 50\mu\text{m}$  grid in each section (Stamataki et al., 2006). Between 9 and 15 sites were counted per cochlea so that each section containing SGNs was represented. The total number of markers was then divided by the product of the grid area and number of sites counted to calculate SGN density. For comparison, two-dimensional SGN density was also calculated using data provided in the SI report. The marker total for each cochlea was divided by product of the number of sites with counts and the two-dimensional area of a single counting site to give the SGN density per  $\mu\text{m}^2$ .

## 3. Results

### 3.1 Stereological SGN Estimates

SGNs were counted using SI software in four cochleae from normal-hearing C57 mice, and population estimates were obtained using the Optical Fractionator probe. Counts were weighted by the measured thickness of each section. The mean estimated population of SGNs in normal-hearing C57 mice was 7009 with a standard deviation of 996. This estimated count using design-based stereology falls within the range of published literature values for mouse SGNs as shown in Table 1. To verify the accuracy of the stereological estimates, a single cochlea was recounted three times using the same counting parameters. The results of these counts show a standard deviation of 368.

To evaluate the sensitivity of design-based stereology to SGN degeneration associated with hearing loss, SGN counts of four cochleae from mice with age-related hearing loss were

obtained using the same parameters in SI. These mice were used in a previous study by Stamatakis et al. (2006) which established that they had age-related hearing loss using auditory brainstem response audiometry. Hequembourg and Liberman (2001) previously documented a significant decrease in SGNs in C57 mice between 3 to 7 months of age. Figure 2 compares sections showing a full complement of SGNs in a normal-hearing C57 mouse and loss of SGNs in a mouse with age-related hearing loss. Although individual neurons are densely packed in normal specimens, they were reliably delineated at 40x magnification with a 10x eyepiece and appropriate light adjustments. The mean estimated SGN population in mice with hearing loss was 5096 with a standard deviation of 713, showing a significant reduction compared to normal-hearing mice (Table 2; student's t,  $p=0.012$ ). The coefficient of variation of the normal-hearing C57 SGN population estimates was 14.21, which was very close to that of old C57 SGN population estimates at 14.00.

### 3.2 SGN Packing Densities

Two-dimensional SGN packing densities were calculated for all four normal C57 cochleae and all four cochleae with hearing loss following the profile counting method described by Stamatakis et al. (2006). The average SGN density of normal-hearing mice measured using a randomly placed  $50\mu\text{m} \times 50\mu\text{m}$  grid was  $3.84 \times 10^{-3}$  SGN/ $\mu\text{m}^2$  and the average density of SGNs in cochleae with hearing loss was  $2.79 \times 10^{-3}$  SGN/ $\mu\text{m}^2$ . Two-dimensional SGN densities were also calculated using data provided in the SI report of population estimates. This method showed an average SGN density of  $4.66 \times 10^{-3}$  SGN/ $\mu\text{m}^2$  in normal-hearing mice, with an average SGN density of  $3.02 \times 10^{-3}$  SGN/ $\mu\text{m}^2$ . The average SGN packing density of normal-hearing mice calculated using the Stamatakis method did not significantly differ from the density calculated from SI data, nor was there a significant difference between the SGN densities of mice with age-related hearing loss as determined by the two methods (Table 3, student's t).

## 4. Discussion

In the present study, we demonstrate that design-based stereology estimates normal mouse SGN populations well within the range of previously published values, and our counts using C57 mice fall between other population estimates for this strain. This method is also sensitive to degeneration of SGNs associated with age-related hearing loss, making it a useful analytical tool in studying hearing loss in a mouse model. Recent studies have chosen to report two-dimensional SGN densities in lieu of estimated SGN population; however, the SI report provides both a population estimate and the data needed to calculate two-dimensional SGN density while requiring approximately the same amount of time to count a single cochlea.

### 4.1 Comparison to other SGN population estimates

Estimates of SGN population in the present study fell within the range counts reported by four other studies using the same strain, Luikart et al. (2003), Agerman et al. (2003), Liebl et al. (1997) and Fariñas et al. (1994). The counts from Liebl et al. are much lower than in other studies, possibly because only nuclei were counted. Differences between our SGN counts and those slightly higher (Johnson et al., 2011; Postigo et al., 2002) may be related to variation in strain. Whitlon et al. (2006) reported counts slightly higher than the median of published values, which is approximately 8041, and this may be accounted for by their method of counting every cell and the outbred strain CD-1. Richter et al. (2011), using the same methods of counting and staining as Whitlon et al., observed much higher populations. This may have to do with differences in animal age or strain. SGN counts reported by Ehret (1979) are among the highest reported values, potentially due to the practice of counting afferent fibers from a cross-section of the cochlear nerve rather than cell bodies, nuclei, or

nucleoli in the spiral ganglion as in other studies. Additionally, Ehret used silver stain, which stains a random subset of cells in their entirety, and cross-sections of the cochlear nerve for analysis. Camarero et al. (2001) obtained counts nearly twice as large as the numbers from other studies. Their parameters,  $ssf=1/2$ ,  $asf=1/10$ , and evaluation interval= $20/48.7\ \mu\text{m}$ , are very close to those used in the present study; however, their counts do not fall as close to the median population estimate for normal-hearing mice. The cause of the discrepancy is unclear.

Individual variability in the size of the cochlea may also account for the range of population estimates from normal mice shown in Table 2. This variability occurs in many previous studies as well, with reported errors ranging from 96 to 1325 (Table 1). Additionally, standard error of the mean (SEM), which is the standard deviation divided by the square root of the sample size, is often listed instead of the standard deviation, lowering the perceived variability of the data. Stereological estimates resulted in similar coefficients of variability for both young and old C57s (Table 2). Two-dimensional densities, computed from SI data and from profile counts, had a wider spread of coefficients of variability in both young and old C57s (Table 3). The differing coefficients of variability of two-dimensional packing densities may indicate another drawback to using these methods since SI population estimates of SGNS in the same mice had more consistent variability.

It is worth mentioning that while the average population estimate given by studies employing serial reconstruction or stereology is higher than that of studies using profile counts in the C57 strain, this does not unequivocally verify the inaccuracy of these profile counts. There is substantial variability in mouse strain and age across studies, and we have very little systematic data comparing SGN counts across strains and age using the same counting methods. Most of the lower population estimates from profile counts use the same strain, C57Bl6, at a very young age. The higher estimates, on the other hand, represent a wide range of mouse strains and ages – often outbred or hybrid strains.

## 4.2 Practical considerations

The setup for stereology requires high-quality objectives, a motorized microscope stage, z-axis recorder, video camera and software, which, though expensive, can be shared among users of a large facility. Though serial reconstruction methods still offer the highest degree of accuracy, stereology should be considered as a replacement for the more prevalent practice of profile counts. As an unbiased technique, design-based stereology yields greater confidence in results that identify significant group differences than do traditional two-dimensional methods while being less time-consuming than counting every cell. Design-based stereology using the optical fractionator, as in this study, requires thick sections (von Bartheld, 2002) and may not be useful for quantifying all sensory and neural components of the cochlea such as hair cells or myelinated fibers of the auditory nerve. Structures for which it would be difficult to obtain a sampling of sections at regular intervals from the entire volume containing the population being estimated, such as nerve fibers, are not ideal for stereology. Stereology is not sensitive to localized cell loss in a particular region of the cochlea; it can only estimate the number of cells in a well-defined, bounded area. Thus, if a particular area of the basilar membrane is under study or if it is necessary to measure the loss of SGNS as a function of distance from either the base or the apex of the cochlea, a three-dimensional reconstruction might be preferred.

It is of note that the two-dimensional densities obtained by profile counts and by SI data are similar; however the two procedures are equally time-consuming, and SI data provides a broader array of information, such as total population, density, and volume of the region of interest. The two-dimensional densities obtained by profile counts also showed a wider range of variability, with coefficients of variation of 12.78 and 28.34 for normal-hearing and

old C57s respectively. The coefficients of variations for SI two-dimensional densities were 21.93 for young C57s and 18.27 for old C57s, and the coefficients of variation for SI population estimates, shown in Table 2, are extremely similar. Some studies (Kujawa and Liberman, 2009; Wang et al., 2002) have opted to calculate a percent SGN loss by counting a single mid-modiolar section and comparing it with baseline mid-modiolar counts. While this takes approximately a third of the time necessary for the methods used in the present study, it is often difficult to obtain a perfect mid-modiolar section, and selection of a region for analysis in this manner is subject to bias. Additionally, a single section is unlikely to reveal abnormalities present in other regions of the cochlea. The reader is referred to Richter et al. (2011) for recommendations relevant to analyzing specific cochlear locations.

### 4.3 Applications

Stereological estimation of SGN population counts has the potential for very broad applications in hearing research since it is intended to count naturally occurring structures of any shape, size or orientation in a given volume. For example, it can be used to count neurons expressing a specific protein using immunohistochemistry or to estimate the population of SGNs displaying visible abnormalities, such as vacuolization or nucleus irregularities. A pilot study must be run for each new structure under investigation to optimize counting frame dimensions, section thickness evaluation interval, and other variable parameters. While the present study quantified SGN loss due to age-related hearing loss, the same method could also be applied to investigate recovery after treatment. Stereology may also be useful for characterizing new genetically engineered strains and can be used with emerging confocal microscope applications and stored three-dimensional image stacks.

### Acknowledgments

The research reported in this publication was supported by the National Institute On Deafness And Other Communication Disorders of the National Institutes of Health under Award Numbers DC012352 and DC005211. The content is solely the responsibility of the authors and does not necessarily represent the official views of the National Institutes of Health. We would like to thank Howard Francis for the use of tissue samples from his lab.

### References

- Agerman K, Hjerling-Leffler J, Blanchard MP, Scarfone E, Canlon B, Nosrat C, Ernfors P. BDNF gene replacement reveals multiple mechanisms for establishing neurotrophin specificity during sensory nervous system development. *Development*. 2003; 130:1479–1491. [PubMed: 12620975]
- Camarero G, Avendaño C, Fernández-Moreno C, Villar A, Contreras J, de Pablo F, Pichel JG, Varela-Nieto I. Delayed inner ear maturation and neuronal loss in postnatal igf-1-deficient mice. *J Neurosci*. 2001; 21:7630–7641. [PubMed: 11567053]
- Dorph-Petersen KA, Nyengaard JR, Gundersen HJG. Tissue shrinkage and unbiased stereological estimation of particle number and size. *J Micro*. 2001; 204:232–246.
- Ehret G. Quantitative analysis of nerve fibre densities in the cochlea of the house mouse (*Mus Musculus*). *J Comp Neurol*. 1979; 183:73–88. [PubMed: 758336]
- Fariñas I, Jones KR, Backus C, Wang XY, Reichardt LF. Severe sensory and sympathetic deficits in mice lacking neurotrophin-3. *Nature*. 1994; 369:658–661. [PubMed: 8208292]
- Francis HW, Ryugo DK, Gorelikow MJ, Prosen CA, May BJ. The functional age of hearing loss in a mouse model of presbycusis. II Neuroanatomical correlates. *Hear Res*. 2003; 183:29–36. [PubMed: 13679135]
- Glueckert R, Bitsche M, Miller JM, Zhu Y, Prieskorn DM, Altschuler RA, Schrott-Fischer A. Deafferentation-Associated Changes in Afferent and Efferent Processes in the Guinea Pig Cochlea and Afferent Regeneration With Chronic Intrascalar Brain-Derived Neurotrophic Factor and Acidic Fibroblast Growth Factor. *J Comp Neurol*. 2008; 507:1602–1621. [PubMed: 18220258]
- Guillery RW. On Counting and Counting Errors. *J Comp Neurol*. 2002; 447:1–7. [PubMed: 11967890]

- Hequembourg S, Liberman CM. Spiral Ligament Pathology: A Major Aspect of Age-Related Cochlear Degeneration in C57BL/6 Mice. *JARO*. 2001; 2:118–129. [PubMed: 11550522]
- Ishiyama G, Geiger C, Lopez I, Ishiyama A. Spiral and vestibular ganglion estimates in archival temporal bones obtained by design based stereology and Abercrombie methods. *J Neuro Methods*. 2011; 196:76–80.
- Johnson SB, Schmitz HM, Santi PA. TSLIM imaging and a morphometric analysis of the mouse spiral ganglion. *Hear Res*. 2011; 278:34–42. [PubMed: 21420476]
- Kujawa SG, Liberman MC. Adding Insult to Injury: Cochlear Nerve Degeneration after “Temporary” Noise-Induced Hearing Loss. *J Neurosci*. 2009; 29:14077–14085. [PubMed: 19906956]
- Lauer AM, Fuchs PA, Ryugo DK, Francis HW. Efferent synapses return to inner hair cells in the aging cochlea. *Neurobiol of Aging*. 2012; 33:2892–2902.
- Li H-S, Borg E. Age-related Loss of Auditory Sensitivity in Two Mouse Genotypes. *Acta Otolaryngol*. 1991; 111:827–834. [PubMed: 1759567]
- Liebl DJ, Tessarollo L, Palko ME, Parada LF. Absence of sensory neurons before target innervation in brain-derived neurotrophic factor-, neurotrophin 3-, and TrkC-deficient embryonic mice. *J Neurosci*. 1997; 17:9113–9121. [PubMed: 9364058]
- Luikart BW, Nef S, Shipman T, Parada LF. In vivo role of truncated TrkB receptors during sensory ganglion neurogenesis. *Neuroscience*. 2003; 117:847–858. [PubMed: 12654337]
- MacDonald GH, Rubel EW. Three-dimensional confocal microscopy of the mammalian inner ear. *Audiol Med*. 2010; 8:120–128.
- MacDonald GH, Rubel EW. Three-dimensional imaging of the intact mouse cochlea by fluorescent laser scanning confocal microscopy. *Hear Res*. 2008; 243:1–10. [PubMed: 18573326]
- Mikaelian DO. Development and Degeneration of Hearing in the C57/bl6 Mouse: Relation of Electrophysiologic Responses from the Round Window and Cochlear Nucleus to Cochlear Anatomy and Behavioral Responses. *The Laryngoscope*. 1979; 1:1–15. [PubMed: 423642]
- Mouton, PR. Principles and Practices of Unbiased Stereology: An Introduction for Bioscientists. Johns Hopkins Press; 2001.
- Ohlemiller KK, Gagnon PM. Genetic dependence of cochlear cells and structures injured by noise. *Hear Res*. 2007; 224:34–50. [PubMed: 17175124]
- Parry-Hill, M.; Sutter, RT.; Davidson, MW. Microscope Alignment for Köhler Illumination. Nikon Microscopy U. 2013. <<http://www.microscopyu.com/tutorials/java/kohler/index.html>>
- Postigo A, Calella AM, Fritsch B. Distinct requirements for TrkB and TrkC signaling in target innervation by sensory neurons. *Genes Dev*. 2002; 16:633–645. [PubMed: 11877382]
- Richter CP, Kumar G, Webster E, Banas SK, Whitlon DS. Unbiased counting of neurons in the cochlea of developing gerbils. *Hear Res*. 2011; 278:43–51. [PubMed: 21329751]
- Shepherd RK, Coco A, Epp SB. Neurotrophins and electrical stimulation for protection and repair of spiral ganglion neurons following sensorineural hearing loss. *Hear Res*. 2008; 242:100–109. [PubMed: 18243608]
- Stamataki S, Francis HW, Lehar M, May BJ, Ryugo DK. Synaptic alterations at inner hair cells precede spiral ganglion cell loss in aging C57BL/6J mice. *Hear Res*. 2006; 221:104–118. [PubMed: 17005343]
- Von Bartheld CS. Counting particles in tissue sections: Choices of methods and importance of calibration to minimize biases. *Histol Histopathol*. 2002; 17:639–648. [PubMed: 11962763]
- Wang Y, Hirose K, Liberman MC. Dynamics of noise-induced cellular injury and repair in the mouse cochlea. *JARO*. 2002; 3:248–268. [PubMed: 12382101]
- Whitlon DS, Ketels KV, Coulson MT, Williams T, Grover M, Edpao W, Richter CP. Survival and morphology of auditory neurons in dissociated cultures of newborn mouse spiral ganglion. *Neuroscience*. 2006; 138:653–662. [PubMed: 16413120]



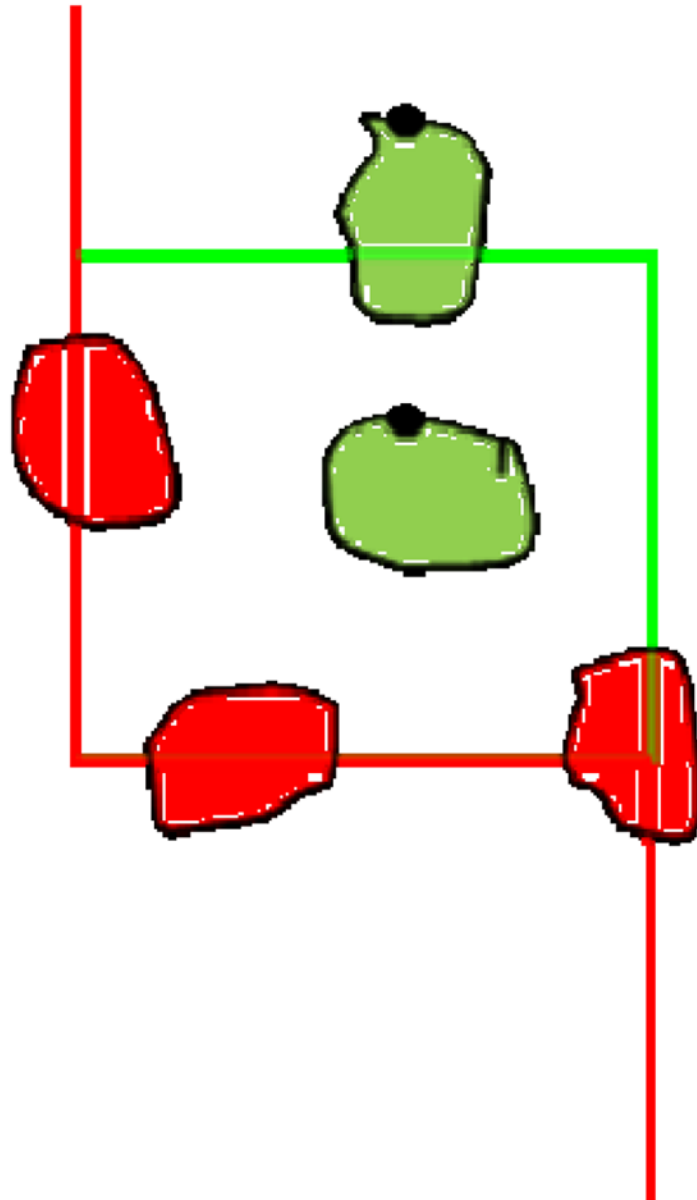


**Figure 1.**

A model of a StereoInvestigator sampling site. Objects of interest fully within the square or touching the green line are marked on a common unique point. In this figure, the tops of the cells are marked with a black dot. Objects of interest outside of the square or touching the red line are not counted.

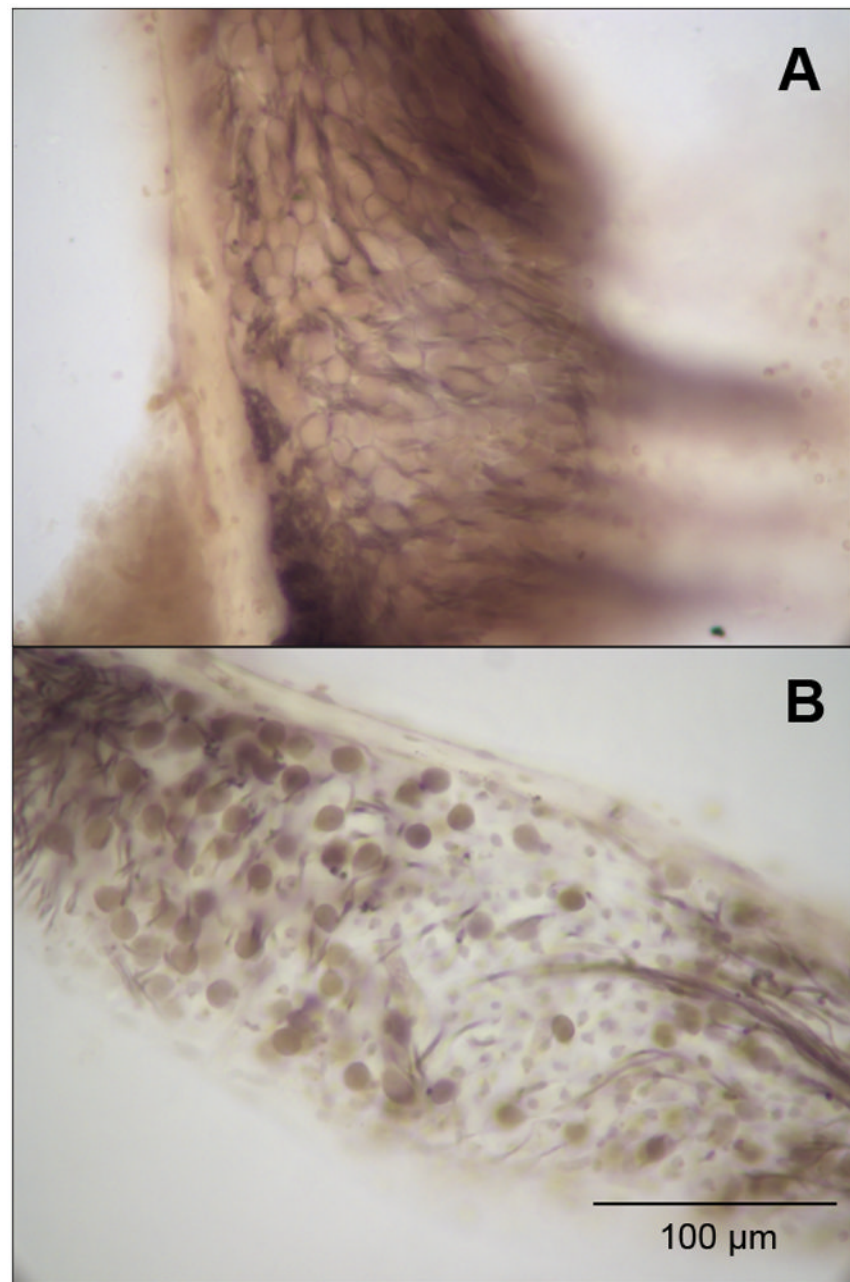


**Figure 2.** C57 mice demonstrate normal hearing thresholds at a young age and develop age-related hearing loss beginning around 3 to 4 months of age. Panel A shows a basal turn of the spiral ganglion at 40x magnification of a young, 11 week-old, C57 with normal hearing. Panel B shows a basal turn of the spiral ganglion at 40x magnification of an old C57 between 8–12 months of age with age-related hearing loss.

Table 1

Published estimated values of mouse SGN populations

Investigator	Strain	Age (days)	Section Thickness ( $\mu\text{m}$ )	Section Sampling Fraction	Structure	Staining Agent	Counting Method	Correction Factor	Spiral Ganglion Neuron Population	Error
Liebl et al., 1997	C57Bl6	0.5	5	Every 6th	Nuclei	Hematoxylin	Profile counts	None	4421	1325 SEM (n=3)
Agerman et al., 2003	C57Bl6	0	14	Every 3rd	Nucleoli	Cresyl violet	Profile counts	Abetcrombie	~6500	~500 SEM (n=4)
Agerman et al., 2003	C57Bl6	17	14	Every 3rd	Nucleoli	Cresyl violet	Profile counts	Abetcrombie	~6800	~300 SEM (n=4)
Present counts	C57Bl6	56-77	40	Every 2nd	Cell bodies	Osmium	Stereology, optical disector	None	7009	996 SD (n=4)
Luikart et al., 2003	C57Bl6	0	8	Every 10th	Cell bodies	Cresyl violet	Profile counts (computer automated)	None	7148	291 SEM (n=5)
Postigo et al., 2002	129 $\times$ C57Bl6	7	8	Every 5th	Nuclei	Cresyl violet	Profile counts	Abetcrombie	~7800	~300 SD (n=3-4)
Postigo et al., 2002	129 $\times$ C57Bl6	70	8	Every 5th	Nuclei	Cresyl violet	Profile counts	Abetcrombie	~8000	~100 SD (n=3-4)
Fariñas et al., 1994	C57Bl6	0	10	Every 6th	Nucleoli	Cresyl violet	Profile counts	None	8082	1132 SEM (n=3)
Whitton et al., 2006	CD-1	1	5	Every cell	Nuclei	Toluidine blue	Reconstruction	None	8240	423 SD (n=3)
Johnson et al., 2011	CBA/JCr	28	5	Every cell	Cell bodies	Rhodamine B isothiocyanate	Reconstruction	None	8626	96 SEM (n=5)
Richter et al., 2011	C57Bl6/129Svj	70	5	Every cell	Cell bodies	Toluidine blue	Reconstruction	None	10402	Not reported
Ehret, 1979	NMRI	28-70	3	25 cross-sections of cochlear nerve	Afferent fibers	Silver nitrate	Profile counts	None	10483	~810 SD (n=6)
Camarero et al., 2001	MF1 $\times$ 129/sv	5	50	Every 2nd	Nuclei	Cresyl violet	Stereology, optical disector	None	16100	700 SD (n=3)
Camarero et al., 2001	MF1 $\times$ 129/sv	20	50	Every 2nd	Nuclei	Cresyl violet	Stereology, optical disector	None	16600	600 SD (n=5)

**Table 2**

Sensitivity of stereological quantification to SGN loss.

<b>Normal-Hearing C57 (8–11 weeks)</b>	<b>Estimated Population using Number Weighted Section Thickness</b>
C57060119	6221
C57060110	6281
C57060112	7187
C57051215	8349
<i>mean ± SD</i>	7009 ± 996
<i>coefficient of variation</i>	14.21
<b>Old C57 (8–12 months)</b>	
Maekin (L)	4206
Maekin (R)	5107
Calvin (L)	5116
Calvin (R)	5953
<i>mean ± SD</i>	5096 ± 713
<i>coefficient of variation</i>	14.00

**Table 3**

Two-dimensional SGN densities by method

	<b>Stamatakis et al. (mean ± SD)</b>	<b>StereoInvestigator (mean ± SD)</b>	<i>significant</i>
<b>Normal-Hearing</b>	$3.84 \times 10^{-3} \pm 4.91 \times 10^{-4}$ SGN/ $\mu\text{m}^2$	$4.66 \times 10^{-3} \pm 1.02 \times 10^{-3}$ SGN/ $\mu\text{m}^2$	No (p=0.100)
<i>coefficient of variation</i>	12.78	21.93	
<b>Age-Related Hearing Loss</b>	$2.79 \times 10^{-3} \pm 7.91 \times 10^{-4}$ SGN/ $\mu\text{m}^2$	$3.02 \times 10^{-3} \pm 5.51 \times 10^{-4}$ SGN/ $\mu\text{m}^2$	No (p=0.326)
<i>coefficient of variation</i>	28.34	18.27	
<i>significant</i>	Yes (p=0.032)	Yes (p=0.015)	